Molecular Orientation in Polyester Films Using Polarized Laser Raman and Fourier Transform Infrared Spectroscopies and X-Ray Diffraction

George Voyiatzis

Foundation for Research & Technology-Hellas, Institute of Chemical Engineering and High Temperature Chemical Processes, P.O. Box 1414, 26500 Patras, Greece

Giorgos Petekidis[†] and Dimitris Vlassopoulos*

Foundation for Research & Technology-Hellas, Institute of Electronic Structure & Laser, P.O. Box 1527, 71110 Heraklion, Crete, Greece

Efstratios I. Kamitsos

National Hellenic Research Foundation, Institute of Theoretical and Physical Chemistry, 48 Vas. Constantinou Avenue, 11635 Athens, Greece

Albert Bruggeman

TNO Plastics and Rubber Research Institute, P.O. Box 6031, 2600 JA Delft, The Netherlands

Received August 16, 1995; Revised Manuscript Received January 2, 1996[⊗]

ABSTRACT: Polarized laser Raman and FTIR spectroscopies, as well as wide angle X-ray diffraction (WAXD), have been employed in order to investigate the distribution of molecular orientation in uniaxially drawn solution-cast films of well-characterized polyesters, bearing hexyl side chains, at different draw ratios. Both the second ($\langle P_2(\cos\theta)\rangle$) and fourth ($\langle P_4(\cos\theta)\rangle$, only with Raman) moments of the segment orientation distribution function have been determined. Results reveal physically meaningful trends of both P_2 and P_4 with draw ratio. A critical comparison among the three techniques confirms the sensitivity of Raman and FTIR to order at molecular level, when detecting the orientation of a particular segment, compared to similar WAXD results that provide information on the larger scale liquid crystalline domain orientation only and thus correspond to higher values of P_2. Therefore, the corresponding dependencies of P_2 on draw ratio are also different. A simplified approach for the analysis of the Raman spectra, based on the cylindrical symmetry of the Raman tensors at a specific vibrational normal mode, demonstrates the effectiveness and usefulness of this technique for accurately and fully determining the molecular orientation in rodlike polymers.

1. Introduction

It is well known that molecular orientation in polymers, induced, for example, by drawing, results in ultrahigh-modulus materials (usually fibers or films).[1−3] This important property is a manifestation of the intrinsic stiffness of polymer chains and is therefore particularly pronounced in semicrystalline and liquid crystalline polymers.[2] The latter, in particular, exhibit significant chain rigidity and might lead to specific moduli comparable to that of steel; consequently, they are extremely interesting materials in terms of industrial applications.[3] This enormous potential of oriented polymers has created the need to accurately characterize the degree of molecular orientation in both the bulk and films, under various processing conditions. Several experimental techniques have been applied to this end,[2,4−7] including birefringence, X-ray diffraction and scattering, infrared dichroism, fluorescence polarization, NMR, dynamic mechanical thermal analysis (DMTA), Raman scattering, and more recently polarization−modulation methods (infrared dichroism or Raman).[8,9] These techniques have been applied extensively to a number of flexible polymers such as polyethylene,[10] polypropylene,[5,11] poly(vinyl chloride),[12] poly(ethylene terephthalate),[13] polystyrene,[14] and poly(methyl methacrylate),[7] as well as to flexible polymer blends.[15] The key message from these investigations is that molecular orientation in flexible polymers (amorphous or semicrystalline) can be determined unambiguously, and thus the effects of deformation on the material's final properties can be assessed.

A special note should be made for the Raman spectroscopy; in addition to its potential (like other techniques) to provide independent information on the average molecular orientation of both amorphous and crystalline phases in a semicrystalline polymer, it enables independent determination of the second as well as the fourth moment of the orientation distribution function; the former is defined as $\langle P_2(\cos\theta)\rangle = [3\langle\cos^2\theta\rangle - 1]/2$ and will be referred to as P_2 in the rest of this paper, whereas the latter is defined as $\langle P_4(\cos\theta)\rangle = [35\langle\cos^4\theta\rangle - 30\langle\cos^2\theta\rangle + 3]/8$ and will be referred to as P_4. Both parameters are necessary in order to fully determine the orientation distribution function and understand the mechanical properties of oriented polymers in terms of molecular models. Moreover, Raman scattering does not impose any geometrical restrictions on the test specimens (as, for example, infrared dichroism does). On the other hand, the analysis of the Raman data is somehow ambiguous and certainly requires a good knowledge of the molecular structure of the system under investigation and a large number of experiments for each orientation (P_2, P_4) data point. In that respect Fourier transform infrared (FTIR) spectroscopy and wide angle X-ray diffraction (WAXD) are quite useful. Both are more straightforward in the analysis and require much less experimental effort, as

[†] Also at the Department of Physics, University of Crete, 71110 Heraklion, Crete, Greece.

[⊗] Abstract published in *Advance ACS Abstracts,* February 15, 1996.

0024-9297/96/2229-2244$12.00/0

Chart 1. Molecular Structure of Polyester PES 3:3/C6

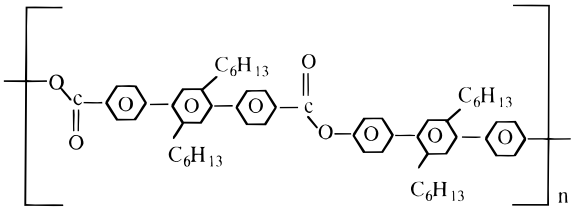

will become evident later; but FTIR provides information only on P_2, whereas the determination of P_4 from WAXD is rather inaccurate.

Orientation phenomena in liquid crystalline polymers have also received a great deal of attention, due to their great potential for industrial applications, mainly the ones associated with fibers and films. Infrared spectroscopy, X-ray diffraction, and DMTA have been the techniques of choice for these materials.[16,17] It is clear that these materials orient much more effectively than their flexible counterparts, but again two types of oriented areas, namely, liquid crystalline and amorphous, may be present, depending on the material's liquid crystalline phase behavior. Several investigators have addressed the effects of draw ratio and geometry. Most of the literature data refer to film or bulk measurements; the former were performed in order to assess the surface-induced orientation.[18] However, no complete analysis of the distribution of molecular orientation has been carried out to date. Further, it should be noted that a complete and detailed quantitative analysis of the molecular orientation of low molecular weight liquid crystalline phases, based on Raman scattering measurements, was performed several years ago;[19] however, Raman scattering has not been used to date to study polymeric liquid crystals.

In this study, laser Raman spectroscopy, FTIR spectroscopy, and WAXD have been utilized in order to quantitatively determine the degree of molecular orientation in uniaxially oriented liquid crystalline films of polyesters, as a function of the draw ratio. The films were produced by solution casting of the polyester in chloroform, at room temperature, and subsequent drawing at high temperature and various draw ratios. Results on the combined information concerning the second and fourth terms of the expansion of the orientation distribution function are discussed both qualitatively and quantitatively. The effect of liquid crystallinity on chain orientation and the distinction between large-scale domain orientation and molecular-level orientation is also addressed. It is shown that the polyesteric films orient very effectively at relatively low draw ratios (compared to the flexible polymers). The combination of the techniques used represents a very powerful tool for a complete quantitative characterization of the molecular orientation in liquid crystalline polymers.

The paper is organized as follows: Section 2 describes the materials and the three experimental techniques utilized. The results, a thorough analysis, and discussion are presented in section 3. Finally, the main conclusions are summarized in section 4.

2. Experimental Section

Materials. A model polyester (PES) with hexyl side chains, synthesized by a polycondensation technique[20] and coded as PES 3:3/C6 was employed. Its chemical structure is shown schematically in Chart 1. Its molecular weight was determined to be about 35 000, based on intrinsic viscosity measurements.[21] This polymer was dissolved in chloroform, at concentrations in the range of 3−6% by weight. Prior to film casting, the solution was filtered on a Teflon filter (5 μm pore size) to remove dust particles. Solutions were then cast on a glass plate at room temperature with 1000 μm blades.[21] Films of nearly uniform thickness (of about 30 ± 2 μm) were obtained after evaporation of the solvent. Uniaxially oriented films were obtained by drawing the PES 3:3/C6 cast films in an oven at a temperature of about 270 °C. The temperature was controlled by passing preheated dry nitrogen gas through the oven. The standard drawing speed was 2 cm/min, and the specimen length and width before drawing were 5 and 1 cm, respectively. The draw ratios achieved were between 1.5 and 3.1. Even by varying the temperature and drawing speed, it was not possible to obtain films at higher draw ratio, due to breaking.[17]

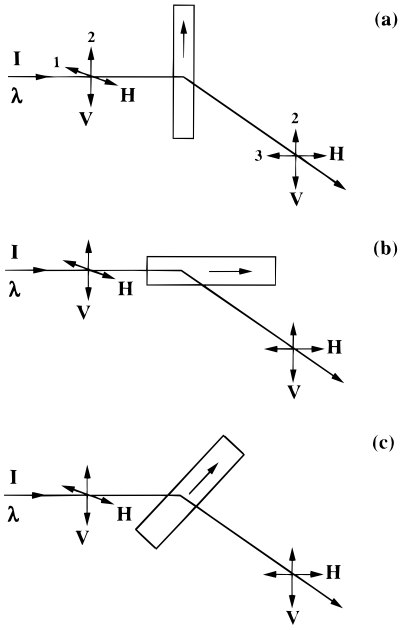

Figure 1. Characteristic scattering geometries for the Raman spectroscopic measurements: (a) perpendicular position of specimen, corresponding to 90° angle between incident laser beam and macroscopic drawing direction, (b) horizontal position of specimen, corresponding to 0° angle between incident laser beam and macroscopic drawing direction, and (c) diagonal position of specimen, corresponding to 45° angle between incident laser beam and macroscopic drawing direction. V and H represent the vertical and horizontal polarization to the scattering plane, respectively, of the incident or scattered laser radiation. Numbers 1−3 refer to the coordinate system of the Raman tensor.

Laser Raman Scattering. The Raman spectra were excited with a Spectra Physics (model 164) argon ion laser using typically 100 mW of the 514.5 nm line. The laser beam was directed at the polyesteric film specimen through an optical train; the latter includes mirrors, iris diaphragms, a narrow band-pass interference filter, a half-wave plate, and a cylindrical lens. The specimen was positioned mechanically at a special stage that can rotate by 360°. The 90° scattered light was collected with a F/1.4 (80 mm diameter) lens at the slit of a monochromator through an analyzer for selecting the appropriate polarization and a quarter-wave plate to compensate for grating polarization preference. A Spex model 1403 double monochromator coupled with an RCA model C-31034 photomultiplier tube (PMT) was used to analyze the scattered radiation. The detection system included Par photon counting and rate meter electronics. The signal from the PMT and the electronics was recorded and analyzed on a personal computer.

Measurements were carried out at three different geometries of the incident laser beam with respect to the drawing direction of the film specimens and the polarization direction (Figure 1). In the first geometry, the drawing direction was perpendicular (90°) to the direction of the incident laser beam; in the second one, it was parallel (0°); finally, in the last one, it was at 45° with respect to the incident laser beam. The reason for choosing this variety of geometries is related to the

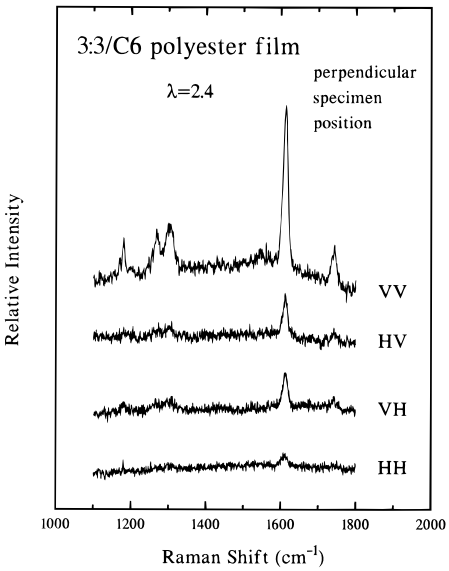

Figure 2. Raman spectra of the PES 3:3/C6 polyester film with perpendicular specimen position and $\lambda = 2.4$.

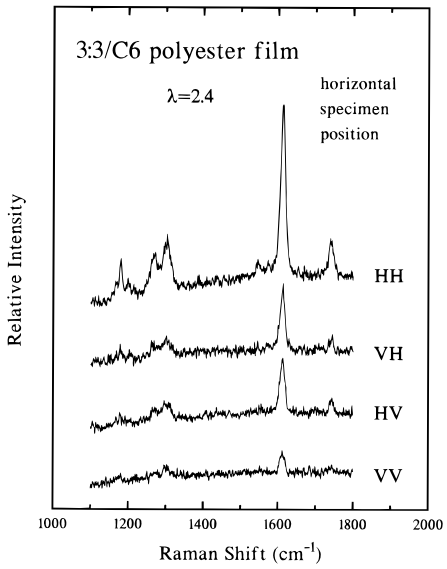

Figure 3. Raman spectra of the PES 3:3/C6 polyester film with horizontal specimen position and $\lambda = 2.4$.

need to obtain specific values of the scattered radiation (as function of the above angle and polarization direction), as dictated by the theoretical requirements for the quantitative determination of the molecular orientation; this will become apparent below and has been addressed in the literature as well.[22,23]

FTIR Spectroscopy. Infrared spectra were measured in the transmission mode on a Bruker vacuum spectrometer (IFS 113v). The sample was mounted with its plane perpendicular to the incident infrared beam. A KRS-5 wire-grid polarizer was positioned before the sample to polarize the infrared radiation. The polarizer remained fixed, and the sample was rotated by 90° in order to obtain transmission spectra with different polarization directions. The transmission spectrum of the polarizer was measured using the same instrument settings and was employed as the reference spectrum. All spectra were measured at room temperature and represent the average of 200 scans at 2 cm^{-1} resolution.

WAXD. Oriented film diffractograms were recorded in transmission mode using Ni-filtered radiation (flat film, sample to film distance 6 cm). The X-ray beam was directed parallel to the film surface. For determining the degree of orientation, a procedure according to Crevecoeur and Groenincx[24] was used. The azimuthal intensity distribution, $I(\phi)$, of the most intense (100) equatorial reflection was established with an ENRAF-Nonius densitometer, via radial scans with a varying step size of 1−5°. Air scattering was substracted after recording a blank diffractogram, and the constant intensity level at high azimuthal angles was taken as material background scattering and substracted from the intensity profile.

3. Results and Discussion

Raman Spectra. Spectra from the PES 3:3/C6 polyesters at various draw ratios λ (1.5, 2, 2.4, 2.6, 2.8, 3.1) and different polarization geometries (VV, VH, HV, HH) were obtained. Results for $\lambda = 2.4$ and the three angles 90°, 0°, and 45° are depicted in Figures 2−4, respectively. Looking at the spectra of Figure 2, it becomes apparent that the peaks are much more pronounced in the VV mode rather than in the HV and HH modes; this means that vibrations along the direction of stretching are much stronger than in the combinations of polarizations and suggests a significant degree of molecular orientation along the stretching direction. Analogous observations hold for Figure 3, where vibrations in the HH mode are more pronounced, while in Figure 4 the intensity of each band remains quite unaffected by changing polarization geometries.

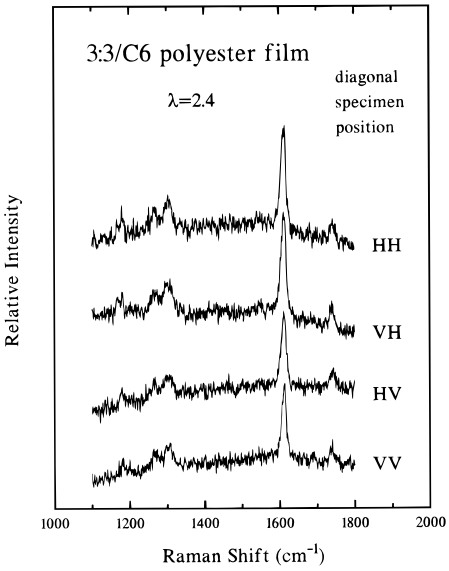

Figure 4. Raman spectra of the PES 3:3/C6 polyester film with diagonal specimen position and $\lambda = 2.4$.

In order to determine the degree of molecular orientation, it is important to focus our attention to a specific Raman band. This was chosen as the 1616 cm^{-1} band, mainly for two reasons: (i) This band is strong and well-resolved, and therefore its intensity can be determined accurately, and (ii) it is a well-known Raman band, attributed to the C═C stretching mode in the C_1-C_4 direction of the benzene ring.[13,25] This direction can vary as much as 6° with respect to the main axis of the macromolecule, as will be discussed later. This peak assignment is of crucial importance for the determination of P_2 and P_4, as will become apparent below. Therefore, in the remaining of the paper, the analysis of the Raman scattering intensities will refer to the 1616 cm^{-1} line. It is now clear how one can estimate the molecular orientation of the polyester films from Figures 2−4 discussed above.

An important implication from these experiments is the determination of the effect of draw ratio on the orientability of the polyester films. This effect is manifested in Figure 5, which represents VV and HV Raman spectra at various draw ratios, λ, for the vertical sample geometry (Figure 1a). One can clearly observe a progressive change of the relative Raman intensities

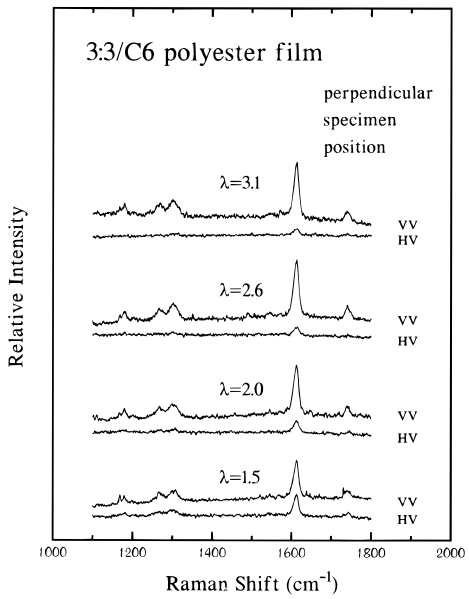

Figure 5. Raman spectra of the PES 3:3/C6 polyester film with perpendicular specimen position, at several draw ratios (1.5−3.1).

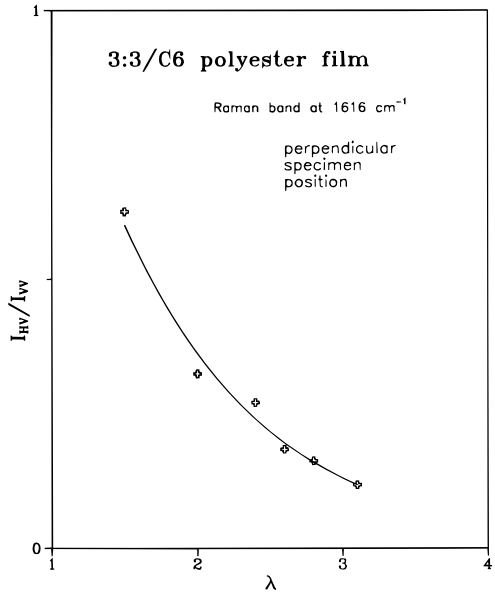

Figure 6. Experimental Raman depolarization ratio (I_{HV}/I_{VV}) of the PES 3:3/C6 polyester film, as a function of draw ratio. The line is drawn to guide the eye.

as the draw ratio varies. Since the depolarization ratio ($\rho = I_{HV}/I_{VV}$) is related to the orientation of the films, one can, in principle, use the linear−linear plot in Figure 6 in order to determine the effect of λ in inducing orientation. This is truly apparent, since the slope of ρ versus λ decreases substantially at the high values of draw ratio; for a perfectly oriented material, we expect the slope to approach zero.

In order to quantify the molecular orientation, we adopt the analysis of Pigeon et al.,[22,23] which is actually a special case of that of Kamitsos and Risen;[26] they are based on the theory of Bower,[27] who has determined the distributions of molecular orientation in oriented polymers from their Raman spectra. Here we summarize the important points of the analysis. The total Raman scattering intensity, I_s, is given by

$$I_s = I_0 \sum_N \left(\sum_{i,j} I_i I_j' a_{ij}\right)^2$$

where I_0 is a constant depending on instrumental factors and the incident light intensity, a_{ij} are the components of the Raman tensor, i and j (each taking values from 1 to 3) refer to axes fixed in the sample, and I_i and I_j' are the directions cosines, which define, respectively, the polarization direction of the incident and scattered light with respect to the axes of the test sample. Summations inside the parentheses are carried out over all i's and j's, whereas summation outside the parentheses represents the contribution of all scattering units, N, to the measured intensity. The experimental values are of the form $I_0\sum a_{ij}a_{pq}$, where each a_{ij} can be expressed as a linear combination of the principal components α_1, α_2, and α_3 of the Raman tensor of the vibration investigated and the Euler angles defining the orientation of the principal axes of the tensor with respect to the axes of the sample. By assuming uniaxial symmetry with no preferred orientation around the main molecular axis, one can write

$$\sum_{i,j,p,q} a_{ij}a_{pq} = 4\pi^2 N \sum_{l=0,2,4} M_{l00}A_{l00}^{ijpq} \qquad (1)$$

where N is the number of structural units contributing to the Raman intensity and A_{l00}^{ijpq} is a sum of quadratic terms in α_1, α_2, and α_3, previously tabulated by Bower.[27] M_{l00} is expressed in terms of Legendre polynomials: $M_{l00} = (1/4\pi^2)\{(2l+1)/2\}^{1/2}\langle P_l(\cos\theta)\rangle$. Under the above assumptions of uniaxial symmetry of the samples, the problem of determining the orientation moments P_l is reduced to a system of five nonlinear algebraic equations for the Raman scattering intensity:

$$I_0\sum a_{22}^2 = b[(3a_1^2 + 3a_2^2 + 3 + 2a_1a_2 + 2a_1 + 2a_2)/15 + P_2(3a_1^2 + 3a_2^2 - 6 + 2a_1a_2 - a_1 - a_2)/21 + 3P_4(3a_1^2 + 3a_2^2 + 8 + 2a_1a_2 - 8a_1 - 8a_2)/280] \quad (2)$$

$$I_0\sum a_{33}^2 = b[(3a_1^2 + 3a_2^2 + 3 + 2a_1a_2 + 2a_1 + 2a_2)/15 - 2P_2(3a_1^2 + 3a_2^2 - 6 + 2a_1a_2 - a_1 - a_2)/21 + P_4(3a_1^2 + 3a_2^2 + 8 + 2a_1a_2 - 8a_1 - 8a_2)/35] \quad (3)$$

$$I_0\sum a_{21}^2 = b[(a_1^2 + a_2^2 + 1 - a_1a_2 - a_1 - a_2)/15 + P_2(a_1^2 + a_2^2 - 2 - 4a_1a_2 + 2a_1 + 2a_2)/21 + P_4(3a_1^2 + 3a_2^2 + 8 + 2a_1a_2 - 8a_1 - 8a_2)/280] \quad (4)$$

$$I_0\sum a_{32}^2 = b[(a_1^2 + a_2^2 + 1 - a_1a_2 - a_1 - a_2)/15 - P_2(a_1^2 + a_2^2 - 2 - 4a_1a_2 + 2a_1 + 2a_2)/42 - P_4(3a_1^2 + 3a_2^2 + 8 + 2a_1a_2 - 8a_1 - 8a_2)/70] \quad (5)$$

$$I_0\sum a_{22}a_{33} = b[(a_1^2 + a_2^2 + 1 + 4a_1a_2 + 4a_1 + 4a_2)/15 - P_2(a_1^2 + a_2^2 - 2 + 10a_1a_2 - 5a_1 - 5a_2)/42 - P_4(3a_1^2 + 3a_2^2 + 8 + 2a_1a_2 - 8a_1 - 8a_2)/70] \quad (6)$$

where $b = I_0N\alpha_3^2$, $a_1 = \alpha_1/\alpha_3$, $a_2 = \alpha_2/\alpha_3$, and $P_2 = \langle P_2(\cos\theta)\rangle$ and $P_4 = \langle P_4(\cos\theta)\rangle$ are as already mentioned. Tensor indices i and j refer to polarization of incident and scattered laser beam, respectively, which are also reflected in Figure 1 (incident, H ↔ 1 and V ↔ 2; scattered, H ↔ 3 and V ↔ 2). The intensities at the left-hand side of eqs 2−6 can be obtained experimentally

by measuring the Raman spectra at various combinations of polarization geometries and angles (γ') between molecular axes and laboratory fixed reference frame (vertical, horizontal, diagonal). Spectra for the same $I_0\sum a_{22}^2$, $I_0\sum a_{33}^2$, $I_0\sum a_{21}^2$, and $I_0\sum a_{32}^2$, respectively, were averaged in order to improve the accuracy of the measurements and minimize birefringence effects;[22] they were obtained by using $\gamma' = 0°$ and $90°$. A special note should be made for the $I_0\sum a_{22}a_{33}$ spectrum. This spectrum could not be measured directly, and it was thus calculated from other spectra ($I_0\sum a_{22}^2$ and $I_0\sum a_{33}^2$) and the HV spectra at $\gamma' = 45°$. The latter involve some inaccuracy due to potential birefringence problems which are likely to occur at 45°. Nevertheless, in similar studies of PET orientation, it was shown[28] that the 1616 cm^{-1} Raman band is only slightly affected by birefringence, and thus the error invloved in our measurements is considered small.

As already mentioned in the Introduction, attempts to solve the equations numerically revealed several problems, due to the fact that, depending on the choice of initial conditions, several acceptable solutions can be obtained.[22,23] This represents a nontrivial problem that cannot be resolved satisfactorily only by mathematical means; it is also imperative to impose the right physical restrictions on the system under investigation, i.e., to understand the structure of the molecular chain and the assignment of Raman lines. To this end a number of crucial boundary conditions and assumptions have been taken into consideration.

(a) Limiting values of the variables were chosen. In particular, $0 < P_2 < 1$, while $-0.39 < P_4 < 1$.[29] Further, the parameter b should be always positive, as implied by the analysis above.

(b) The 1616 cm^{-1} line of the benzene ring vibration (C_1-C_4) was used in our calculations for the following reasons: (i) it is the strongest line in the Raman spectrum, (ii) it occurs as an isolated and well-localized line in the Raman spectrum of para-disubstituted benzene ring, with very small changes of frequency observed in a variety of related "model" compounds,[30,31] as also confirmed by vibrational calculations,[30] and (iii) it is not directly affected by conformational changes[32] and is expected to give a reliable indication of the overall chain orientation.[33] Thus, it is very likely that one of the principal components of the Raman tensor coincides with the chain axis for this vibration (the deviation, estimated to be about 6° [21] on the average, is considered very small, since it does not change the resulting P_2 values significantly; this is also supported from literature data on PET with the same Raman band,[13,25,28] where for a deviation of about 19°, the results were not much affected). Finally, and most importantly, symmetry considerations mentioned below are crucial to the choice of this specific Raman band.

(c) The Raman tensor of the 1616 cm^{-1} line was assumed cylindrical, i.e., $a_1 = a_2$; this means that the two components of the polarizability tensor perpendicular to the plane of the ring and perpendicular to the C_1-C_4 direction are of the same sign and magnitude. Due to symmetry considerations, this assumption is viewed as legitimate. Moreover, it was also justified in numerous studies of PET reported in the literature;[13,25,28] in particular, ref 25 is important, since it clearly shows that a comparison of orientation moments calculated with and without the assumption of uniaxial Raman tensor leads to the conclusion that the assumption is reasonable. Since the above is true, for an angle between the C_1-C_4 direction in the benzene ring and the chain axis direction of about 19°,[13] it is safe to make the same assumption for the 6° case. Using the above considerations, it is straightforward to simplify the original system of five equations and end up with

Table 1. P_2 and P_4 Values Determined from Raman Scattering Measurements (1616 cm^{-1})

	draw ratio					
	1.5	2.0	2.4	2.6	2.8	3.1
P_2	0.19	0.42	0.54	0.56	0.66	0.68
P_4	−0.30	0.06	0.20	0.21	0.21	0.37

$$P_2 = \frac{(-x^2 - 2x)M - 1 + 4x}{(-x^2 + x)M + 4x - 4} \tag{7}$$

$$P_4 = \frac{(8x^2 - 16x + 8)Q - 64x^2 - 32x - 24}{(8x^2 + 8 - 16x)(2 + Q)} \tag{8}$$

$$b = \frac{f}{\frac{8x^2 + 3 + 4x}{15} + P_2\frac{8x^2 - 6 - 2x}{21} + P_4\frac{24x^2 + 24 - 48x}{280}} \tag{9}$$

where

$$M = \frac{8h - g}{k - w}$$

$$Q = \frac{2f + g}{2k + h}$$

and f, g, h, k, and w are the experimental Raman scattering intensities (as functions of γ' and polarization) $I_0\sum a^2_{22}$, $I_0\sum a^2_{33}$, $I_0\sum a^2_{21}$, $I_0\sum a^2_{32}$, and $I_0\sum a_{22}a_{33}$, respectively. Further, $x = a_1$ (under the assumption $a_1 = a_2$) and is determined from the depolarization ratio, ρ, of the isotropic sample:[7,28]

$$\varrho = (1 - x)^2/[8x^2 + 4x + 3] \tag{10}$$

Results based on the above simplified approach are presented in Table 1. A few remarks are in order: First of all, it is noted that the negative value P_4 at $\lambda = 1.5$ can be explained as in ref 29, i.e., it corresponds to a distribution of C_1-C_4 vibrations in which all chain axes lie on a cone of angle α such that $P_2(\cos\alpha) = P_2$. As seen in Table 1, the results follow the right qualitative trend, as suggested by Figure 6, and are also in quantitative agreement with orientation results on similar systems.[16,18] This represents a first qualitative test of the reliability of the above approach for analyzing the Raman data and determining the molecular orientation. It should be also noted that the values of P_4 fall within the acceptable range, for a given P_2 value, according to the analysis of Bower[29] for uniaxially oriented polymers; this represents another confirmation of the consistency of the methodology employed here.

Infrared Spectra. The usefulness of the FTIR absorption measurements in determining molecular orientation originates from the fact that the infrared absorption of a characteristic group of the polymer is given by:

$$A \propto \left(\frac{\partial \boldsymbol{\mu}}{\partial r}\cdot\mathbf{E}\right)^2 = \left(\frac{\partial \mu}{\partial r}E\right)^2 \cos^2\gamma \tag{11}$$

where $\partial\boldsymbol{\mu}/\partial r$ is the transition dipole moment, $\mathbf{E}$ is the electric field of the infrared radiation, and γ is the angle between the dipole moment and the electric field. It is

evident that maximum absorption is obtained when the radiation is polarized parallel to the dipole moment that develops during the vibration of a characteristic group, while no absorption will be measured for perpendicular polarization. For a random distribution of orientations of the absorbing group and, therefore, random orientation of the resulting dipole moments, the measured infrared absorption will be independent of polarization, whereas when there is partial alignment, the absorption will depend on polarization of the infrared radiation. Therefore, by using linearly polarized infrared light, the orientation of the functional groups of a polymer can be studied.

The absorption anisotropy is expressed by the dichroic ratio, D, defined as:

$$D = \frac{A_{\parallel}}{A_{\perp}} \tag{12}$$

where $A_{\parallel}$ and $A_{\perp}$ are the absorptions measured with the incident radiation being polarized parallel and perpendicular, respectively, to a reference direction. For the case of polymers, the reference direction is usually the draw direction. The average of the second-order Legendre polynomial, also known as the Hermans−Stein orientation function of polymer chains, can be calculated from dichroic measurements by using the relationship:[34]

$$P_2 = \frac{(D-1)(D_o+2)}{(D+2)(D_o-1)} \tag{13}$$

where $D_o = 2\cot^2\psi$ is the dichroic ratio for perfect orientation, with ψ the angle between the direction of the vibrational transition moment and the polymer chain axis. For vibrations for which $\psi = 90°$, eq 13 reduces to

$$P_2 = 2(1-D)/(D+2) \tag{14}$$

while for $\psi = 0°$ one obtains,

$$P_2 = (D-1)/(D+2) \tag{15}$$

Therefore, the second moment of the orientation function can be calculated from polarized infrared measurements.

Such measurements were performed on the same samples employed for the Raman study. Figures 7 and 8 depict the polarized absorption spectra obtained from the PES 3:3/C6 samples with $\lambda = 1.5$ and 3.1, respectively. As shown in these figures, a number of infrared bands exhibit saturation effects when the radiation is polarized parallel to the stretching direction of the film. This is attributed to a combined effect resulting from the relatively large film thickness (about 30 μm) and the strong absorption by the film under parallel polarization of radiation.

Like in the Raman investigation, we employ sensitive probe bands to quantify the molecular orientation induced by stretching. In the spectral region typical of CC stretching vibrations of the aromatic rings, four bands are observed at 1485, 1510, and 1605 cm^{-1}, all of which exhibit parallel dichroism. We focus on the band centered at 1605 cm^{-1} because (i) this band is well resolved from the other CC components and (ii) it appears to be the infrared counterpart of the 1615 cm^{-1} Raman. Indeed, the para-disubstituted benzene ring of PES 3:3/C6 has no center of symmetry, and therefore,

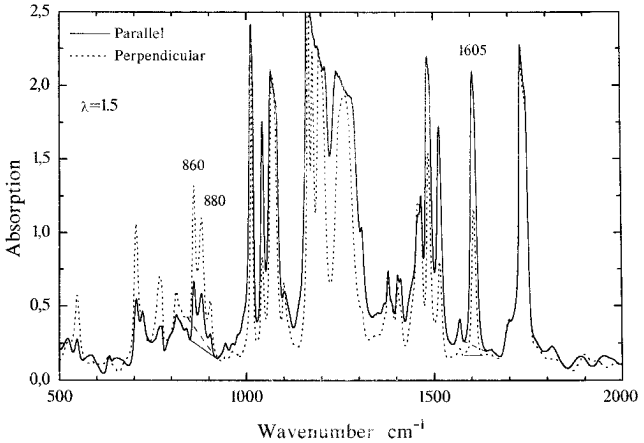

Figure 7. Polarized infrared absorption spectra for the PES 3:3/C6 polyester film at draw ratio $\lambda = 1.5$. Solid lines represent polarization parallel to the stretching direction; dashed lines represent polarization perpendicular to the stretching direction. Base lines for the peaks at 860 and 1605 cm^{-1} are drawn.

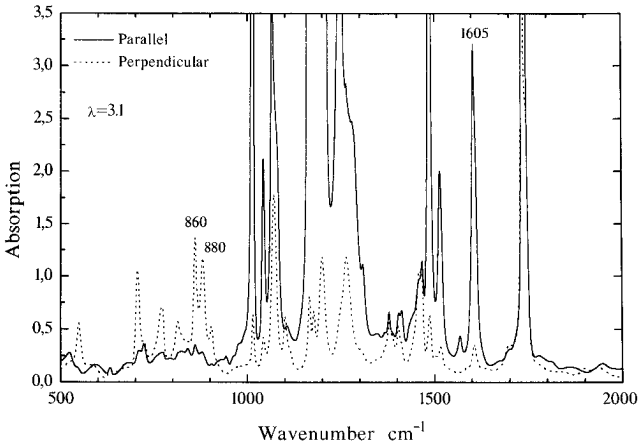

Figure 8. Polarized infrared absorption spectra for the PES 3:3/C6 polyester film at draw ratio $\lambda = 3.1$. Solid lines represent polarization parallel to the stretching direction; dashed lines represent polarization perpendicular to the stretching direction.

the mode giving rise to the Raman band at 1616 cm^{-1} becomes infrared active as well.[35] There are other examples of polymeric materials containing para-disubstituted benzene rings with no center of symmetry that exhibit strong infrared bands at 1605 cm^{-1} with parallel dichroism.[18,36] On these grounds we assign the infrared band at 1605 cm^{-1} to the C═C stretching vibration in the C_1-C_4 direction, in analogy with the Raman band at 1615 cm^{-1}.[25] The dichroic ratio, D, for the 1605 cm^{-1} band was determined by the base-line method,[37] and is plotted in Figure 9 versus draw ratio. Values of D were obtained for three samples only, with $\lambda = 1.5$, 2.6, and 3.1, because all other samples showed saturation of the 1605 cm^{-1} band in the parallel polarized spectra. A systematic increase of D with draw ratio is evident from Figure 9 (in comparison to Figure 8). Assuming that the dipole moment for the 1605 cm^{-1} band is parallel to the C_1-C_4 direction, and therefore parallel to the chain axis of the polymer, the trend of D suggests the development of chain axis orientation along the stretching direction. Under the assumption that $\psi = 0°$, eq 15 can be used to calculate P_2 for the 1605 cm^{-1} band. The results are given in Table 2. Comparisons with the corresponding P_2 values obtained from the Raman analysis (Table 1) show similar results and the same trend with draw ratio. This observation confirms the fact that the two techniques are probing the same

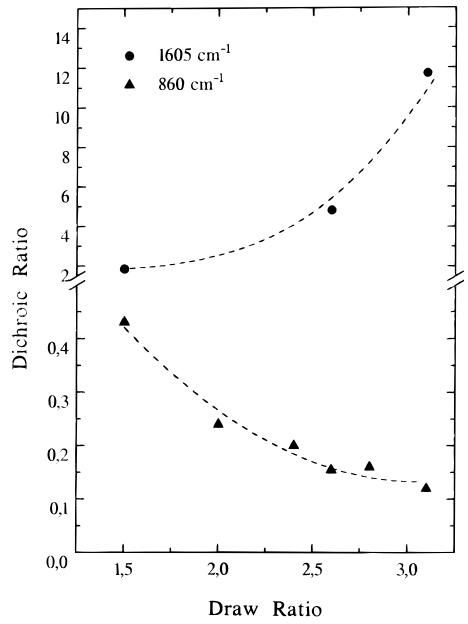

Figure 9. Dichroic ratios for the 860 (bottom) and 1605 (top) cm^{-1} infrared bands as a function of draw ratio. Lines are drawn to guide the eye.

Table 2. P_2 Values Determined from FTIR Measurements

	draw ratio					
	1.5	2.0	2.4	2.6	2.8	3.1
P_2 (1605 cm^{-1})	0.22			0.56		0.78
P_2 (860 cm^{-1})	0.47	0.68	0.73	0.78	0.78	0.83

molecular mode and therefore orientation, as will be discussed below.

Besides the 1605 cm^{-1} band, other infrared bands can also be used to investigate the tendency for molecular orientation in the polyester films. Of particular interest is the doublet at 860 and 880 cm^{-1}, which exhibits polarization opposite to that of the 1605 cm^{-1} band. This doublet can be assigned to the C−H out-of-plane bending vibration of the benzene rings, with transition moment developing perpendicular to the plane of rings and therefore to the polymer axis.[18,35] This fact explains the opposite polarization found to be exhibited by the 1605 cm^{-1} band and the 860 and 880 cm^{-1} doublet. The dichroic ratio of the stronger component at 860 cm^{-1} was determined and is shown in Figure 9. The progressive decrease of D with λ is another manifestation of the induced molecular orientation upon stretching. Setting $\psi = 0°$ for the vibrational mode giving rise to the 860 cm^{-1} band, we calculate the corresponding P_2 for this mode by using eq 14. The results are included in Table 2. The increase of P_2 with draw ratio is well demonstrated, as in the case of the 1605 cm^{-1} band. The fact that the two bands give different values of P_2 at each λ is not unexpected, since they originate from vibrational modes of different segmental units of the polymer. Similar effects have also been observed in cases of other oriented polymers, including PVC[37] and polypropylene films.[38]

Another source for the difference between the P_2 values of the 860 and 1605 cm^{-1} bands could be traced to the possibility that the corresponding transition moments are not exactly perpendicular and parallel, respectively, to the molecular chain axis. The direction of the dipole moment for the 860 cm^{-1} band is defined rather well, i.e., $\psi = 90°$;[18,35] thus we may assume that $\psi \neq 0°$ for the 1605 cm^{-1} band. Then the orientation function for the molecular chains, $P_{2,\text{chain}}$, can be obtained in terms of the dichroic ratio of the 1605 cm^{-1} band, D, from the expression (eq 16) below, where ψ is the angle between the direction of the transition moment of the 1605 cm^{-1} band and the chain axis:

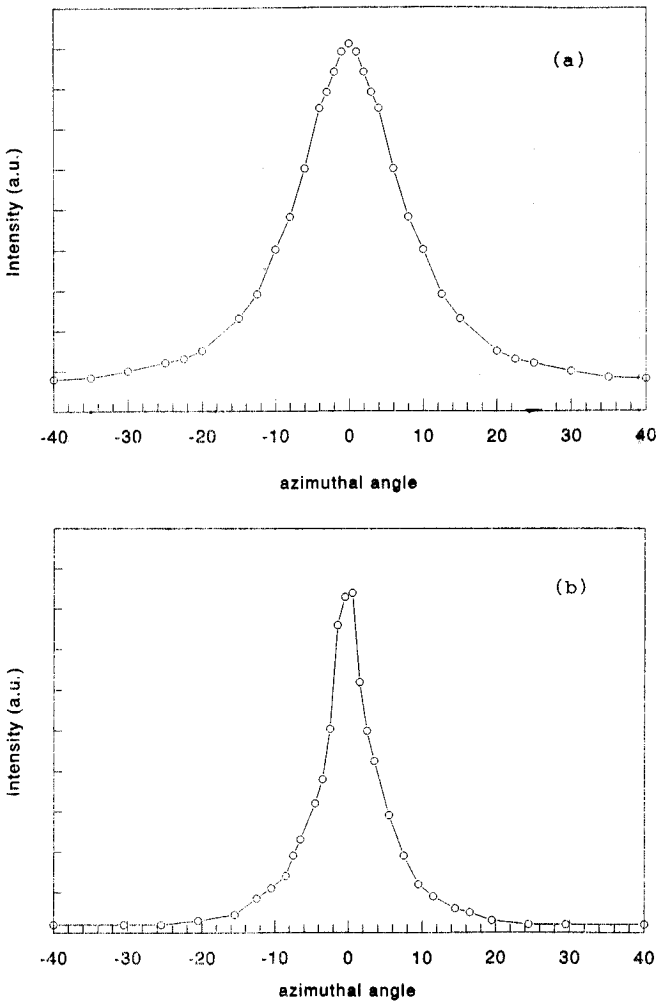

Figure 10. Azimuthal intensity distributions for the PES 3:3/C6 polyester film, obtained by WAXD: (a) $\lambda = 2.0$ and (b) $\lambda = 3.1$.

$$P_{2,\text{chain}} = 2\left(\frac{D-1}{D+2}\right)\left(\frac{1}{3\cos^2\psi - 1}\right) \qquad (16)$$

Assuming that at the highest draw ratio, $\lambda = 3.1$, $P_{2,\text{chain}}$ can be approximated by the P_2 value of the 860 cm^{-1} band ($P_2 = 0.83$ from Table 2), then from eq 16 and the value of D at 1605 cm^{-1} (11.7), we get $\psi = 11.5°$. This result suggests that the assumption made earlier that $\psi = 0°$ is not unreasonable, and in any case, it does not affect the trend of P_2 at 1605 cm^{-1} with draw ratio.

WAXD Results. The WAXD experimental intensity profiles of drawn tapes are convolutions of the orientation distribution and the scattering of a perfectly aligned system. Since the profile of a perfectly aligned system is not known, the narrowest peak obtained (width about 5°) represents an upper limit of this profile, while its lower limit is set by a width of 0°. Deconvolution can be performed according to a procedure of Alexander[39] and assuming a Lorentz shape for all profiles. The degree of orientation was quantified by the full width at half-maximum (fwhm) of the (100) reflection. Typical results are depicted in Figure 10a,b for draw ratios 2.0 and 3.1, respectively. From the azimuthal intensity distributions, $I(\phi)$, the second moment of the orientation distribution was calculated by a numerical integration according to:

$$\langle \cos^2 \theta \rangle = \frac{\int_0^{\pi/2} I(\phi) \cos^2 \phi \sin \phi \, d\phi}{\int_0^{\pi/2} I(\phi) \sin \phi \, d\phi} \qquad (17)$$

The P_2 values thus determined are shown in Table 3 together with the fwhm values. The X-ray P_2 values shown here are calculated assuming a "perfect width" of 0°. Taking into account a "perfect" profile of a few degrees width would lead to systematically higher values of P_2. The presented values exhibit a very small, but nevertheless clear, increase of P_2 with draw ratio (the corresponding dependence of fwhm on draw ratio is more pronounced, as seen in Table 3). It is evident, however, that there exist significant differences with the Raman and FTIR P_2 values, both in magnitude and trend, especially at lower draw ratios. The calculation of orientation parameters from WAXD intensity distributions will be addressed in more detail in a subsequent paper.[21] Here we use the WAXD data only for comparisons and for establishing trends of molecular orientation.

Evaluation of Results. A compilation of the orientation data of the PES 3.3/C6 films obtained with the three techniques is presented in Figure 11. Concerning P_4, the only conclusion that can be drawn is that it follows the right qualitative trend with draw ratio and its values fall within the acceptance range,[29] as already discussed; no further analysis can be made since there is no relevant information from FTIR or WAXD. Concerning P_2, it is very encouraging to note the excellent agreement between the Raman and FTIR data when the same vibrational mode is probed. This is important since both spectroscopic techniques provide information on the molecular orientation by probing essentially the same band, namely, the one originating from the C=C vibration of the phenyl rings. Further, given the fact that the FTIR analysis, with all simplifications made as discussed above, is rather straightforward, the results suggest that the simplified analysis used for the Raman scattering data is indeed unambiguous and highly effective.

As far as the WAXD data are concerned, it is clear that a significant discrepancy exists. This observed discrepancy, which amounts up to 30%, is too large to be accounted for by experimental uncertainties. We believe that it is justified by the fact that Raman and FTIR, which are sensitive to the vibration of a particular group, measure the average molecular orientation, while the WAXD orientation information originates mainly from the liquid crystalline domains (larger entities). More than that, the polyester studied in this work is a material of rather small persistence length[20] and forms a far from perfect liquid crystalline domain, in lyotropic phases. In our case this happens as the solvent is evaporated during film casting. Thus, Raman and FTIR determine the orientation in small areas frozen in from liquid crystalline phase at some temperature, associated with observation on a molecular level (provided of course that the relative position between the vibrational groups probed and the main molecular axis is known). This is what we call "molecular orientation". On the other hand, WAXD looks at layer reflections, which are associated with much larger entities, and refers to the orientation of domains or crystallites, comprising of more than one molecule. This can be considered as a kind of supramolecular domain orientation. It is clear that the order within the layers can be low, whereas the layers relative to each other are highly oriented. In view of this qualitative model, the data of Figure 11 can be understood, and the true effect of draw ratio on molecular orientation can be explained. More specifically, a 100% increase in the draw ratio leads to an over 250% increase in the value of P_2 of the 1616/1605 cm^{-1} band and a corresponding one of 77% for the 860 cm^{-1} band. It is noted that, despite the difference in magnitudes of the 1605 and 860 cm^{-1} bands, the trends are the same. Further, it is remarked that the significantly different magnitude and dependence of WAXD and Raman/FTIR data on the draw ratio confirm that these two approaches look at different kinds of orientation. It should be mentioned that somehow similar explanations, based on a two-domain amorphous−liquid crystalline model, have already been presented in the literature[22,23,40] for other polyesteric materials, in order to explain similar discrepancies. This provides further justification for our interpretation, since these materials form apparently a far from perfect, fully liquid crystalline domain in lyotropic phases. Nevertheless, despite the stability of the presented Raman-based methodology for extracting P_2 and P_4 (due to the assumptions made, results do not depend on any choice of initial conditions, as in previous works[22,23] dealing with the solution of the system of five nonlinear eqs 2−6 above), and the accuracy of the data presented, it is clear that more work is needed in the direction of the proposed model, mainly through theoretical support.

The existing models are mostly developed from continuum mechanical considerations. In particular, the affine deformation model of Kratky[41] can represent, to a good approximation, the orientation of rigid rods in a viscous matrix. The same essentially model was used by Kuhn and Grun in order to describe the orientation of aggregates of anisotropic polymer segments.[42] The model assumes that uniaxial deformation takes place by rotation of chains (or segments) under unconstrained conditions, while elongation may arise only from rotation but not from shear. Under these conditions, the model predicts the second moment of the orientation

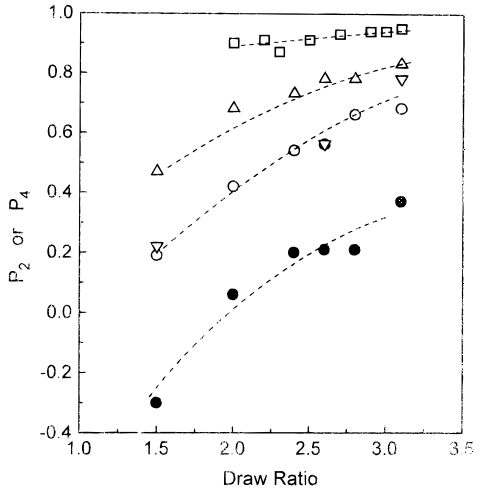

Figure 11. Second and fourth moments of the orientation distribution function, determined from Raman (P_2 and P_4), FTIR (P_2), and WAXD (P_2) measurements: (○) P_2 Raman (1616 cm^{-1}); (▽) P_2 FTIR (1605 cm^{-1}), (●) P_4 Raman (1616 cm^{-1}), (△) P_2 FTIR (860 cm^{-1}), and (□) P_2 WAXD. Lines are drawn to guide the eye.

Table 3. P_2 and fwhm Values Determined from WAXD Measurements

	draw ratio							
	2.0	2.2	2.3	2.5	2.7	2.9	3.0	3.1
P_2	0.90	0.91	0.87	0.91	0.93	0.94	0.94	0.95
fwhm (deg)	15	14	12.6	14.3	13.1	11.8	8	6.7

distribution function as a function of draw ratio only. The agreement with the Raman and FTIR 1616/1605 cm^{-1} data is very good, but one should be careful in evaluating this, since the model does not contain any molecular parameter, and in that respect it is of little value for the present purposes. Another model of relevance is the rubber network model of Roe and Krigbaum.[43] It describes the deformation of a cross-linked network, where the cross-links can be considered as entanglements between chains. This model, however, has some inherent physical limitations when associated with the current rigid-rod polyesters; moreover, it considers the number of links per chain, N_0, as the adjustable parameter. In other words, it predicts P_2 as a function of N_0 and λ. It can predict the Raman data with a decent accuracy when $N_0 = 2$ and the WAXD data when $N_0 = 0.1$. Both values are considered as rather unrealistic. On these grounds, we believe that the rubber network model is not directly correlated to uniaxially oriented rigid-rod macromolecules. It is clear, however, that more work is needed in this direction.

4. Conclusions

Polarized Raman and FTIR spectroscopies have been successfully utilized in order to determine the molecular orientation of polyester films as a function of draw ratio. Results support the idea that while the liquid crystalline domains, probed by WAXD, are highly oriented even at low draw ratios, and depend on them very weakly, the smaller scale average molecular orientation inside these domains is smaller and depends on the draw ratio considerably. Raman scattering is a powerful tool for the determination of both the second and fourth moments of the segment orientation distribution function, when physical considerations regarding the structure of these materials are properly taken into account. A simplified approach for the analysis of the Raman spectra, based on the cylindrical symmetry of the Raman tensors at a specific vibrational normal mode, demonstrates the effectiveness of Raman spectroscopy for quantitative determination of the molecular orientation in rodlike polymers. Agreement between Raman and FTIR data is remarkable, manifesting the reliability of both techniques. Further, for these latter techniques, the effect of draw ratio on increasing molecular orientation is drastic. The combination of all three techniques provides a complete picture of the orientation in rigid-rod polymers. Finally, it is proposed that incorporation of polarization modulation techniques will make measurements faster and interpretation much easier, since the resulting equations are much simpler[9] and require less restrictions than in the present case. This is the subject of future investigations in this direction.

Acknowledgment. The financial support of the European Community, Program BREU, Contract CT910505, is gratefully acknowledged. D.V. would like to acknowledge helpful discussions with Professor S. H. Anastasiadis. The assistance of Mr. Y. Yiannopoulos with infrared measurements is greatfully acknowledged. A.B. is indebted to Dr. J. A. H. M. Buijs for helpful discussions and comments.

References and Notes

(1) Ward, I. M. *Structure and Properties of Oriented Polymers*; Applied Science Publishers: London, 1975.
(2) Ward, I. M. *Developments in Oriented Polymers - I* ; Applied Science Publishers: London, 1982.
(3) Zachariades, A. E.; Porter, R. S. *The Strength and Stiffness of Polymers*; Marcel Dekker: New York, 1983.
(4) Ward, I. M. *Advances in Polymer Science*; Springer-Verlag: Berlin, 1985; Vol. 66, p 81. Ward, I. M. *Developments in Oriented Polymers - II*; Applied Science Publishers: London, 1982.
(5) Lafrance, C.-P.; Prud'homme, R. E. *Polymer* **1994**, *35*, 3927. Gustafsson, G.; Inganas, O.; Osterholm, H.; Laakso, J. *Polymer* **1991**, *32*, 1574.
(6) Jasse, B.; Tassin, J. F.; Monnerie, L. *Progress Colloid Polym. Sci.* **1993**, *92*, 8. Kaito, A.; Kyotani, M.; Nakayama, K. *J. Polym. Sci. B: Polym. Phys.* **1993**, *31*, 1099.
(7) Purvis, J.; Bower, D. I. *Polymer* **1974**, *15*, 645.
(8) Buffeteau, T.; Desbat, B.; Besbes, S.; Nafati, M.; Bokobza, L. *Polymer* **1994**, *35*, 2538.
(9) Archer, L. A.; Fuller, G. G.; Nunnelley, L. *Polymer* **1992**, *33*, 3574. Archer, L. A.; Fuller, G. G. *Macromolecules* **1994**, *27*, 4359.
(10) Lafrance, C.-P.; Chabot, P.; Pigeon, M.; Prud'homme, R. E.; Pezolet, M. *Polymer* **1993**, *34*, 5029.
(11) Satija, S. K.; Wang, C. H. *J. Chem. Phys.* **1978**, *69*, 2739.
(12) Robinson, M. E. R.; Bower, D. I.; Maddams, M. F. *J. Polym. Sci., Polym. Phys. Ed.* **1978**, *16*, 2115. Lauchlan, L.; Rabolt, J. F. *Macromolecules* **1986**, *19*, 1049. Voyiatzis, G.; Papatheodorou, G.; Kamitsos, E. I.; Chrysikos, G.; Anastasiadis, S. H.; Fytas, G. Manuscript in preparation.
(13) Purvis, J.; Bower, D. I.; Ward, I. M. *Polymer* **1973**, *14*, 398.
(14) Jasse, B.; Koenig, J. L. *J. Polym. Sci., Polym. Phys. Ed.* **1978**, *16*, 2115.
(15) Li, W.; Prud'homme, R. E. *Polymer* **1994**, *35*, 3260. Abtal, E.; Prud'homme, R. E. *Polymer* **1993**, *34*, 4661.
(16) Kaito, A.; Nakayama, K.; Kyotani, M. *J. Polym. Sci. B: Polym. Phys.* **1993**, *29*, 1321.
(17) Damman, S. B.; Mercx, F. P. M.; Lemstra, P. J. *Polymer* **1993**, *34*, 2726.
(18) Kaito, A.; Kyotani, M.; Nakayama, K. *Macromolecules* **1991**, *24*, 3244.
(19) Jen, S.; Clark, N. A.; Pershan, P. S.; Priestley, E. B. *J. Chem. Phys.* **1977**, *66*, 4635.
(20) Tiesler, U.; Pulina, T.; Rehahn, M.; Ballauff, M. *Mol. Cryst. Liq. Cryst.* **1994**, *243*, 299.
(21) Bruggeman, A.; Buijs, J. A. H. M.; Damman, S. B. Data to be published.
(22) Pigeon, M.; Prud'homme, R. E.; Pezolet, M. *Macromolecules* **1991**, *24*, 5687.
(23) Citra, M. J.; Chase, D. B.; Ikeda, R. M.; Gardner, K. H. *Macromolecules* **1995**, *28*, 4007.
(24) Crevecoeur, G.; Groenincx, G. *Polym. Compos.* **1992**, *13*, 244.
(25) Lapersonne, P.; Bower, D. I.; Ward, I. M. *Polymer* **1992**, *33*, 1266.
(26) Kamitsos, E. I.; Risen, W. M., Jr. *J. Chem. Phys.* **1983**, *79*, 477.
(27) Bower, D. I. *J. Polym. Sci., Polym. Phys. Ed.* **1972**, *10*, 2135.
(28) Purvis, J.; Bower, D. I. *J. Polym. Sci., Polym. Phys. Ed.* **1976**, *14*, 1461.
(29) Bower, D. I. *J. Polym. Sci., Polym. Phys. Ed.* **1981**, *19*, 93.
(30) Boerio, F. J.; Bahl, S. K.; McGraw, G. E. *J. Polym. Sci., Polym. Phys. Ed.* **1976**, *14*, 1029.
(31) Ward, I. M.; Wilding, M. A. *Polymer* **1977**, *18*, 327.
(32) Cunningham, A.; Ward, I. M.; Willis, H. A.; Zichy, V. *Polymer* **1974**, *15*, 749.
(33) Lewis, E. L. V.; Bower, D. I. *J. Raman Spectrosc.* **1987**, *18*, 61.
(34) Fraser, R. D. B. *J. Chem. Phys.* **1953**, *21*, 1511. Fraser, R. D. B. *J. Chem. Phys.* **1956**, *24*, 89. Stein, R. S. *J. Polym. Sci.* **1958**, *31*, 335. Krimm, S. *J. Polym. Sci.* **1964**, *C7*, 3.
(35) Colthup, N. B.; Daly, L. H.; Wiberley, S. E. *Introduction to Infrared and Raman Spectroscopy*; Academic Press: New York, 1975.
(36) Lei, H.; Zhao, Y. *Polymer* **1994**, *35*, 104.
(37) Jabarin, S. A. *Polym. Eng. Sci.* **1991**, *31*, 638.
(38) Karacan, I.; Taraiya, A. K.; Bower, D. I.; Ward, I. M. *Polymer* **1993**, *34*, 2691.
(39) Alexander, L. E. *X-ray diffraction methods in polymer science*; Wiley: New York, 1969.
(40) Kaito, A.; Kyotani, M.; Nakayama, K. *J. Polym. Sci. B: Polym. Phys.* **1993**, *31*, 1099.
(41) Kratky, O. *Kolloid Z.* **1933**, *64*, 213.
(42) Kuhn, W.; Grun, F. *Kolloid Z.* **1942**, *101*, 248.
(43) Roe, R. J.; Krigbaum, W. R. *J. Appl. Phys.* **1964**, *35*, 2215.

MA951199G